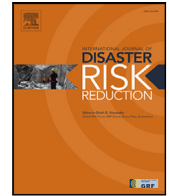




Contents lists available at [ScienceDirect](https://www.sciencedirect.com)

International Journal of Disaster Risk Reduction

journal homepage: www.elsevier.com/locate/ijdr

Modeling potential fire spread polygons and networks for suppression strategies

Minho Kim ^a , Marc Castellnou ^b, Marta C. González ^{c,d,e} ,*

^a Department of Landscape Architecture and Environmental Planning, University of California, Berkeley, 94720, CA, United States

^b Forest Actions Reinforcement Group (GRAF), Catalan Fire Service, Avinguda de Serra Galliners, 112, Cerdanyola del Vallès, 08290, Barcelona, Spain

^c Department of Civil and Environmental Engineering, University of California, Berkeley, 94720, CA, United States

^d Department of City and Regional Planning, University of California, Berkeley, 94720, CA, United States

^e Lawrence Berkeley National Laboratory, Berkeley, 94720, CA, United States

ARTICLE INFO

Dataset link: <https://previncat.ctfc.cat/>, <https://www.meteo.cat/observacions/xema/dades>, <https://github.com/fire2a/C2F-W>, <https://github.com/mbartos/pysheds>, <https://github.com/Deltares/pyflwdir>, <https://github.com/humnetlab/firepolygons>

Keywords:

Fire potential polygons
Spatial networks
Simulation of fire spread
Prescribed burns
Fire suppression
Risk management

ABSTRACT

Unprecedented fire seasons are overwhelming fire suppression capacity in Mediterranean Europe. Fire services respond to urgent risks, but are being outpaced by more complex wildfires. Fire suppression needs proactive and risk-informed strategies to avoid catastrophic wildfires. In this study, we present an automatic method for generating potential fire polygons by adapting hydrological basin delineation techniques to fire spread simulations. Using the time since ignition as input, we segment the landscape into polygons representing discrete spatial units of fire potential. These polygons are then connected into a spatial network, where edges are characterized by penetration rate of spread – a novel metric weighted by the spatial extent of fire spreading between polygons. We apply this method in the field during two major wildfires in Catalonia (Spain) during the 2024 fire season. In the Ciutadilla fire driven by wind, our approach identified high-risk polygons and fire pathways that closely aligned with real suppression actions. In the Vilanova de Meià fire, we implemented different scenarios and modeled their fire potential networks. We demonstrated how proactive tactics and prescribed burn significantly delayed fire progression. Reactive tactics provided minimal benefit. Our approach automates the traditionally manual process of drawing fire potential polygons. In addition, fire potential networks provide crucial information in relation to risk on high-risk polygons, major fire pathways, and potential fire openings. As wildfires continue to threaten our built and natural environments, the proposed method can be integrated into risk-based frameworks to streamline fire management and support proactive strategies.

1. Introduction

Fire is a natural phenomenon in Mediterranean landscapes, intertwined with anthropogenic activity and climate interactions [1, 2]. In recent years, fires have grown larger, hotter, and spread closer to the wildland urban interface [2–6]. Fire suppression has been the main response to managing wildfire emergencies [7]. While only a few extreme fires escape [8], the consequences can be catastrophic. Recent catastrophic wildfires have led to record-breaking loss of human life and infrastructure [9].

In Mediterranean Europe, extreme fires and prolonged fire seasons have overwhelmed the capacity of fire services in recent years [9,10]. Fire services are pressured to respond to urgent risks [7]. Short-term containment may be prioritized given the

* Corresponding author.

E-mail address: martag@berkeley.edu (M.C. González).

<https://doi.org/10.1016/j.ijdr.2025.105853>

Received 17 May 2025; Received in revised form 11 September 2025; Accepted 3 October 2025

Available online 9 October 2025

2212-4209/© 2025 Elsevier Ltd. All rights are reserved, including those for text and data mining, AI training, and similar technologies.

high stakes [11]. However, this view overlooks the uncertainty and potential risks that could exacerbate the wildfire [7,10,11]. As fires grow more complex and unpredictable, this reactive approach is unsustainable and perpetuates a cycle of ineffective suppression [7,8]. In response, fire management needs to adopt proactive, risk-informed strategies [12–15].

1.1. Spatial tools for wildfire risk management

Numerous decision-making support systems and spatial tools have been developed to support fire suppression and management. These tools leverage an interdisciplinary suite of knowledge such as fire spread simulations, GIS, decision science, operations research, and landscape analysis [16]. In particular, spatial tools in wildfire risk management frameworks partition the landscape into spatial units (i.e., polygons) based on suppression difficulty [17], potential control location [12], landscape values [18], and other wildfire risk metrics [19]. In the U.S., the Potential Operation Delineations (PODs) framework was developed for pre-fire planning and risk management [13]. PODs are first built as polygons with boundaries based on potential control locations on the landscape. The boundaries are refined through public workshops and expert knowledge. Quantitative wildfire risk assessments are then used to allocate strategic responses for each POD. However, PODs do not consider the potential spread of fire from one polygon to another. Furthermore, PODs do not dynamically reflect decision-making outcomes such as gaining time, delaying fire spread, and reducing fire intensity. This information is critical to assess the impact of decision-making (successes and failures) and respond accordingly. By understanding the interaction between polygons, users can better understand “where” and “how” the fire is expected to spread.

The Catalan Fire Service developed an approach that segments the landscape into fire potential polygons [15]. Fuel maps, digital elevation models (DEMs), weather data, and expert knowledge of fire behavior are used to qualitatively determine the potential spread from polygon to polygon (henceforth, polygon–polygon connections) [15]. The polygon–polygon connections present opportunities to slow down or stop the progression of fire [7]. Across a large landscape, these connections can be imagined like a connected network. Fire suppression tactics can then target specific connection(s). Existing polygons can be updated dynamically (i.e., re-drawn) according to the fire’s movement and implemented suppression tactics. In practice, these polygons are drawn manually by fire analysts using GIS software and other visualization programs. Polygons boundaries are drawn at potential control lines or where there is a potential change in fire behavior (e.g., roads, bare soil, non-fuels). However, the manually drawing process can be time-consuming and tedious. The polygons neglect spatial topology and are mainly used for visualization. Further, polygons drawn by different users will vary depending on the analyst’s expertise, knowledge of the study area, and data availability. Considering the heightened urgency and stress during wildfire operations, streamlining this manual process is highly desired to eliminate subjective bias and provide essential information for more impactful decision-making [7,15].

1.2. Spatial decision support for fire suppression

In this study, our aim is to develop an automatic method that generates fire potential polygons and spatial networks to support decision-making during fire suppression. To this end, we ask the following questions:

1. How can fire potential polygons be generated automatically?
2. How can connections between polygons be defined?
3. How can the proposed spatial network be utilized to simulate suppression tactics and inform decisions?

First, we need a better understanding of the fire’s intended path and behavior. Fire spreads in the head direction (dominant spread), flank (left and right sides), and back. Fire spread simulations can help model fire propagation to understand fire behavior. For instance, the Minimum Travel Time (MTT) algorithm in FLAMMAP is a widely used 2D fire growth model installed in simulators such as Short Term Fire Behavior in WFDSS, FSPPro, and FSim [20]. These simulators produce pathways with minimum fire spread time from an ignition source based on semi-empirical fire spread simulations. Fire pathways from multiple simulations can also be aggregated to produce burn probability [21]. However, MTT simulations use constant wind and weather conditions for the duration of a single simulation. In this study, we use Cell2Fire, a cellular automata-based semi-empirical fire growth model [22] which uses time-varying weather conditions per time-stamp and landscape input data to simulate fire spread.

Second, we need to automate the generation of fire potential polygons in a tractable and robust way. Many wildfire risk management frameworks in the literature have used the watershed or sub-basin as a spatial unit (i.e., polygons) [13,23,24], especially since DEMs and hydrologic unit maps are readily available. One option is to use object-based image analysis, which clusters similar pixels based on spatial and spectral information into spatial objects [25,26]. However, the spatial objects may be difficult to interpret, especially for users without image processing expertise. Spatial regionalization and optimization techniques are also available [27,28], but may not be suitable for real-time decision-making during fire suppression. Here, we introduce a segmentation method inspired by hydrological basin delineation to automate the generation of fire potential polygons. Concretely, we use a basin delineation algorithm and adapt the logic for fire spread. In basins, water flows from upstream tributaries at a higher elevation to a common outlet downstream. However, fire spread is more complex and discontinuous. To adapt, we use *elapsed time* since ignition as the input variable instead of elevation. We then model the fire’s spread direction (flow direction), accumulation of fire spread paths (flow accumulation), and fire spread order (stream order) to segment fire potential polygons (basins).

In the remainder of the article, Section 2 provides background information on case studies of two wildfires that occurred in Catalonia (Spain) during the 2024 fire season. Section 3 describes the required data input and generated output for our proposed

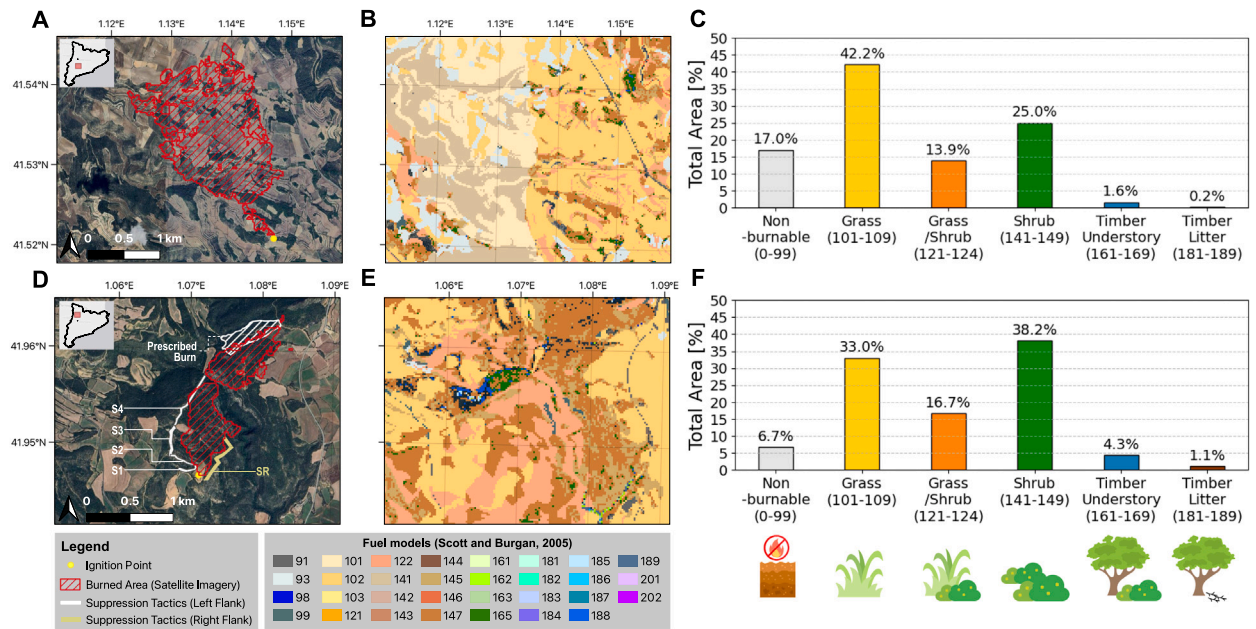


Fig. 1. Area of case studies and landscape characteristics using 40 fuel models [29]. (A) Map of the 2024 Ciutadilla fire showing the burned area (red outline) from satellite measurements. (B) Map of fuel models found in the Ciutadilla landscape. (C) Distribution of fuel models in the Ciutadilla landscape. (D) Map of the 2024 Vilanova de Meià fire showing the burned area (red outline) from satellite measurements with different suppression tactics (E) Map of fuel models in the Vilanova de Meià landscape. (F) Distribution of fuel models in the Vilanova de Meià landscape.

method. We also describe how we process fire spread simulations, fire potential polygons, and fire potential networks for decision-making. We then present the results of the two case studies in Section 4. The first case study focuses on the creation of fire potential polygons and network. The second case study integrates real tactics (fire suppression and pre-fire prescribed burn) into the simulation, and analyzes the resulting polygons and network. We compare the automated and manual polygons and show photos taken during the fire. From the results, we provide guidance on how users can leverage our proposed method for wildfire risk management and tactical decision-making. We provide useful discussion points in Section 5 and summarize the study with concluding remarks in Section 6.

2. Study area and study cases

We apply our proposed method on two case studies of wildfires shown in Fig. 1. In the first case study (see Fig. 1A–C), the fire occurred on 31 July 2024 at 12:37 in an agricultural field in the municipality of Ciutadilla, Lleida province. This region is predominantly filled with low load, dry climate grasses (36.3%), moderate load, dry climate grass–shrub (13.2%), and very high load, dry climate shrub (12.7%). The fire started in cereal fields and quickly spread northwest due to high wind gusts, low humidity, and high temperatures. In two hours, the head fire was not growing significantly and the flank and back were being controlled. However, spotting ignited new fires in forested areas to the northwest. Strong south-southeasterly winds fueled these ignitions, creating multiple active fronts. Further, the fire service expected around two weeks of intensified fire weather. Under these conditions, the fire could cross the C-14 highway in the northeast (see Fig. 1B) and spread uncontrollably in valleys of dense forests and about 1,300 ha of land. If the fire continued spreading, about 5,000 ha of scattered farmland and towns could also burn. Hence, the potential damage would be catastrophic. To avoid this worst-case scenario, the key objectives were twofold: (1) To mitigate widespread fires which would overly strain the fire service’s capacity and resources and (2) to avoid the fire from crossing the C-14 highway. In response, aerial drops (i.e., fire retardants) slowed the fire’s main progression (north) and delayed new fires from spreading in the flank (east and west). Tractors were used to plow the fields ahead of the fire’s right flank (i.e., east) to ensure the fire did not cross the highway. This fire break would stabilize the fire within the extents of the crop fields. The remaining efforts focused on slowing the left flank (i.e., west) to avoid the fire from growing into a larger conflagration. The fire stopped growing and was controlled after almost seven hours and burned around 209 ha of land.

In the second case study (see Fig. 1D–F), a vegetation fire started on 11 August 2024 at 15:23 in a field located in La Noguera, which rapidly spread into the forested areas. The fire burned for around four and a half hours and about 68 ha of land. The study area is mainly filled with low load, dry climate grasses (28.1%), high load, humid climate shrub (11.9%), moderate load, humid climate timber–shrub (11.6%), moderate load, dry climate grass–shrub (11.0%), and moderate load, humid climate timber–grass–shrub

(10.5%). The main priority was containing the head fire using aerial drops and manual tools. The study area is situated in the slopes between the arid Ebro basin and the Pyrenees, where the dry shrubs and grass fuels coexist with sub-humid understory fuels. In this region, June and July are dry months, while August brings storms and horizontal precipitation from fog. These conditions result in dry grasses and brush in the open landscape, whereas the oak and pine forests in the area maintain a sub-humid understory with various fuel types that can survive the arid period. Initially, government officials and local community members were concerned that the fire would spread east and southeast toward nearby towns such as Vall-Llebrera, Artesa de Segre, Alertorn. The fire service reacted to this initial response, as shown by the yellow outlines (“SR”) on the fire’s right flank in Fig. 1D. However, the greatest concern for fire managers was the fire escaping and spreading north and northeast toward Montargull. This was considered to be the worst-case scenario. There were large valleys of dense forest and vegetation that could lead the fire burning uncontrollably. Moreover, it was difficult to suppress the fire’s right flank any further because the head fire’s intensity pushed northeast and limited accessibility. A proactive strategy was imperative. In response, the fire service deployed fire engines and water hose lines to suppress the fire’s left flank. This tactic would avoid possible fires from opening and propagating north/northeast (See suppression tactics “S1” to “S4” in Fig. 1D). In addition, the fire service leveraged a previous prescribed burn area in the northeast (See Fig. 1D) to help slow the fire’s progression and limit the fire’s intensity. Ultimately, this response highlighted the importance of proactive decision-making to avoid excessive damage and uncontrollable fire spread.

Through the second case study, we show how fire potential polygons and networks are updated based on tactic interventions. We represent the suppression tactics and prescribed burn area as vector data (i.e., polygon shapefile). We then update the input fuel maps for the fire spread simulations. Cells affected by suppression tactics are converted to non-fuels. Cells in the prescribed burn area are assigned a low load fuel type (i.e., low load compact conifer litter fuels).

3. Data and methods

3.1. Fire spread simulations

Cell2Fire is an open-source, cell-based fire growth simulator that uses semi-empirical fire spread models [22]. The simulator was designed based on the Canadian Fire Behavior Prediction system and a fuel management and planning framework to mitigate detrimental effects of large-scale fires. Cell2Fire also provides multiple benefits over other simulators, such as dynamic updating of cell states during simulation, incorporating stochastic ignition and weather conditions, adding uncertainty and adjustments of rate of spread (ROS), a parallel processing option, optimization modules, and various visualization outputs [22]. Cell2Fire has been used in Canada [22], Spain [30], US [31], and Chile [32]. Cell2Fire has been compared with multiple widely-used simulators (e.g., FARSITE, Prometheus) and evaluated on real fires, and is determined to be a fast, efficient, and effective model [22]. Cell2Fire can be accessed at <https://github.com/cell2fire/Cell2Fire>.

Cell2Fire intakes regularly-sized grids of fuel models [29], topography (elevation, slope, aspect), and canopy (canopy height, canopy base height, canopy bulk density, canopy cover), as well as weather variables (e.g., wind speed, wind direction, fuel moisture content) defined at regular temporal intervals. All input raster datasets are downloaded from PREVINCAT (<https://previncat.ctfc.cat/>) at 20-m spatial resolution, which provides data for homogeneous fire regime zones [10,33]. Weather data (i.e., wind speed, wind direction, fuel moisture) is acquired from automatic weather stations by the Meteorological Service of Catalonia (<https://www.meteo.cat/observacions/xema/dades>). The ignition point for the simulations is supplied by the fire analyst on duty. The input datasets and weather information used in our two case studies are shown in Figs. S1 and S2 in the Supplementary Materials. [In this study, we use Cell2Fire adapted for Mediterranean landscapes [30,31]. Cell2Fire simulation outputs are generated as grids. Simulated outputs include ROS [m/min], flame length (FL) [m], and fireline intensity (FLI) [kW/m]. More information on Cell2Fire’s spread logic is provided in Section S1 of the Supplementary Materials.

For the Ciutadilla fire, we conduct Cell2Fire simulations for nine hours (two hours longer than the real fire) to view the fire’s potential behavior and spread beyond the highway in the northeast. We set the fuel moisture content to moderately dry based on the scenarios in [29]. For the Vilanova de Meià fire, we execute Cell2Fire simulations for eight hours using the moderately dry fuel moisture content scenario [29]. We consider the strategic scenarios shown in Fig. 1D: (1) No suppression; (2) Prescribed burn; (3) Reactive strategy (Prescribed burn and “SR” tactics); and (4) Proactive strategy (Prescribed burn and “S1–S4” tactics). In general, reactive tactics focus on immediate fire behavior and are deployed directly at or near the visible flame front, aiming to stop or slow the current fire spread where it is actively threatening people, structures, or assets. These tactics are driven by short-term urgency and decision-making prioritizes immediate containment and protection. Proactive tactics focus on potential fire behavior and risk management for strategic containment of the evolving fire. These tactics may not suppress every visible fire, but indirectly address the growing fire to avoid potentially worse outcomes while considering system-wide risk management. Decision-making thus leverages risk information to enhance the safety and effectiveness of suppression.

3.2. Generation of fire potential polygons

Unlike the flow of water, fire spread is not continuous nor cumulative due to variations in the fire behavior, fuels, topography, and wind conditions. Instead of directly using fire spread, we use the *elapsed time* since ignition. Applying a basin delineation algorithm produces a polygon boundary (i.e., basin) containing fire spread paths measured cumulatively over time (i.e., upstream tributaries) since ignition (i.e., outlet point). To help visualize this adapted logic, we illustrate the fire spread simulation and hydrology-inspired modeling of fire potential polygons in Fig. 2. We also provide a 3D visualization of elapsed time in Fig. S3 in the Supplementary

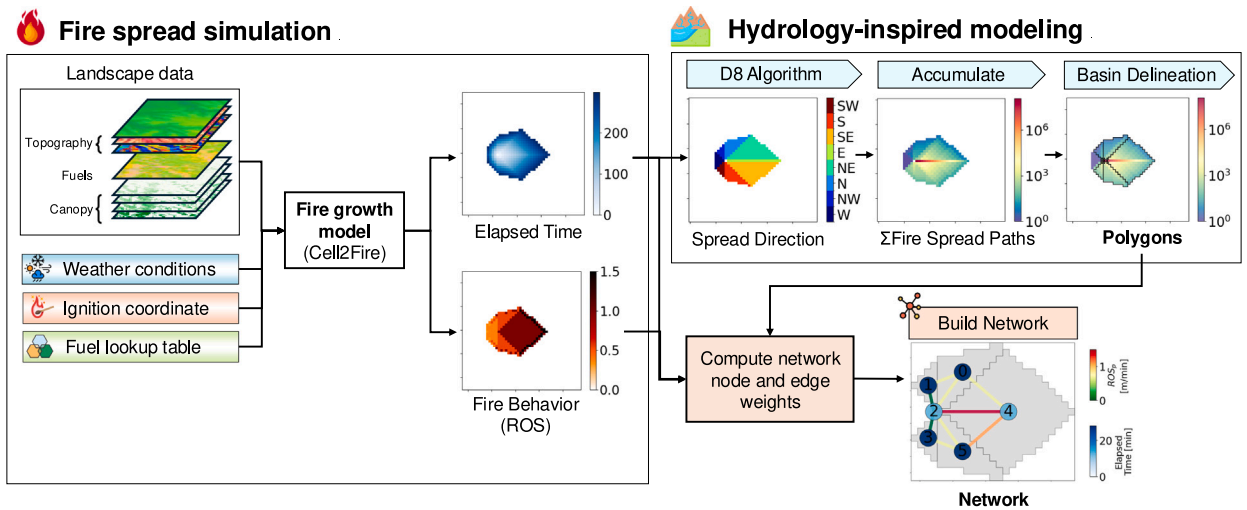


Fig. 2. Diagram of proposed methodology using fire spread simulations and hydrology-inspired modeling of fire potential polygons to build fire potential networks for decision support.

Materials. We provide a comparison of the terminology used in hydrology to delineate basins and our adapted approach for modeling fire potential polygons in Table S2 in the Supplementary Materials. Fire potential polygons are created using elapsed time as the input and intermediate products:

- **Elapsed time** is used as input. For each burned cell, Cell2Fire records the time elapsed for the fire to arrive. Time is measured cumulatively since ignition for the simulation.
- **Fire spread direction** (i.e., flow direction) is computed using the D8 algorithm in the *pysheds* Python package [34]. The D8 algorithm uses an iterative moving window to compute the gradient of a grid's center cell to its neighboring eight cells. The direction of the center cell is determined by the maximum gradient and mapped using an orientation key [35]. This ensures that the fire spread directions are oriented from the ignition point towards maximum elapsed time in the simulation.
- **Cumulative fire spread paths** or Σ spread paths (i.e., flow accumulation) is computed using fire spread direction. This product is calculated by the number of cells that burned earlier (i.e., upstream cells) that have propagated over time from the ignition source.
- **Spread order** (i.e., stream order) is also computed using fire spread direction, where the fire's main and branching fire pathways are identified.

Fire potential polygons are generated from the Σ spread paths by adapting the Pfafstetter basin coding algorithm [36]. Originally, the Pfafstetter coding system was developed to map sub-basins, inter-basins, and isolated regions while maintaining the drainage topology from the largest four sub-basins. The Pfafstetter system has been widely used to map basins worldwide such as the HydroBASINS dataset [37]. For our method, we adopt the Pfafstetter algorithm in the *PyFlwDir* Python package to delineate fire potential polygons. Our adapted Pfafstetter algorithm uses three main parameters: (1) Number of initial largest fire potential polygons; (2) threshold for minimum area of polygons; and (3) threshold for minimum fire spread order.

Adapted Pfafstetter algorithm: First, we start by identifying the ignition cell(s) where elapsed time is assumed to originate from (i.e., outlet points). The algorithm then identifies the largest initial fire potential polygons (i.e., sub-basins) based on areas that burned earlier in time (i.e. upstream areas). Next, the algorithm iteratively searches fire pathways earlier in time (i.e., upstream branches) to identify candidate fire potential polygons. Once all the fire potential polygons are identified, we remove insignificant holes and overly small polygons by merging with adjacent polygons. For further processing, the polygon boundaries can be refined manually by using potential control locations, suppression opportunities, high-value assets, known risks, and other strategic objectives [18].

3.3. Generation of polygon networks

The fire potential polygons are connected into a network. Network nodes are characterized by the average elapsed time and edges are weighted by the fire behavior between polygons. To characterize the edges, we propose a metric called penetration ROS (ROS_p). This metric measures the potential for the fire to spread across polygon boundaries. To compute ROS_p , we use fire spread vectors generated from Cell2Fire simulations. These vectors are created when fire spreads successfully from one cell (centroid) to its neighbor cell (centroid). Fire spread vectors are buffered by half the cell resolution to approximate homogeneous spread between adjacent cells [22]. Subsequently, we overlay the buffered fire spread vectors with the fire potential polygons and find all overlapping

segments. We divide the total length of all overlapping segments by the total perimeter of the polygon boundary. This ratio is the penetration ratio (i.e., proportion of the polygon boundary that can be penetrated by fire spread paths) which is then multiplied by the average ROS (ROS_{avg}), as defined in Eq. (1):

$$ROS_p = \left(\frac{\sum_{i=1}^N L_i}{L_b} \right) \cdot ROS_{avg} \quad (1)$$

where L_i is the length of the polygon's boundary overlapped by the i th fire spread vector, N is the total number of fire spread vectors intersecting the polygon boundary, L_b is the total perimeter of the polygon boundary between a pair of polygons, and ROS_{avg} is the average ROS of fire spread vectors crossing the boundary. ROS_p is especially useful to measure changes in fire spread from suppression tactics and mitigation efforts. The penetration ratio ($\sum_{i=1}^N L_i$) accounts for the spatial extent and ROS_{avg} considers the fire behavior. This metric is computed in the two case studies to build the polygon network used for decision-support and planning suppression strategies. While we use ROS in this study, the edges could also be weighted using other fire behavior metrics such as FLI and FL.

To extract major fire pathways (i.e., fastest spreading paths), we run a shortest path algorithm using elapsed time. We then use a breadth-first search algorithm with a depth limit to compute cumulative ROS_p for all resulting paths and arrange them in descending order. From this list, we extract the top paths (i.e., highest cumulative ROS_p) as major fire pathways.

3.4. Quantitative evaluation

In general, the fire potential network provides useful visual information for decision-makers. The network can be used to identify high-risk connections and polygons, potential opening of fire pathways and cascading effects, and overall fire behavior across the landscape. This information is crucial to help prioritize tactics, allocate resources, and manage uncertainty in the decision-making process. To assess the impact of different suppression tactics, we measure the time gained from a tactic with respect to the baseline scenario (i.e., "No suppression"). Gaining time is crucial to improve the probability of successful initial attack and firefighter safety. More time relates to less heat flux and intensity. More time also translates into more opportunities to plan and prepare. For operations, additional time helps decision-makers adjust strategies and position firefighters to work in a safer, more reliable, and effective manner.

Our intention with the quantitative evaluation is not to suggest that one method is superior, but rather to highlight differences in spatial coverage, suppression difficulty, and alignment with observed fire behavior. Previously, this process was conducted manually by fire analysts and was often subjective. The manual polygons thus represent one possible realization which requires expert judgment, local knowledge, and data availability. Here, we offer an objective and replicable methodology through which the automatic polygons help to expedite, streamline, and standardize the manual process. Given the context where mission and command (with a focus on objectives) are paramount, our proposed methodology facilitates this transition to an automated, standardized approach.

We compare our fire potential polygons with manually-drawn polygons that were used in real-time for the two case studies. We also compare the polygons with the actual burned area data. We extracted burned area via Google Earth Engine by computing the differenced normalized burn ratio from Sentinel-2 satellite imagery acquired before and after the fire. We assess the polygon overlap with the actual burned area. In addition, we consider how local fuels, topography, and suppression conditions can influence the difficulty of suppressing fire. We compute the terrestrial suppression difficulty index ($tSDI$) [17,38], which is measured as a multi-criteria metric by combining indexes of surface fire energy behavior, accessibility based on road distance, penetrability considering terrain conditions, and fireline opening based on fireline production rates using hand and machine tools [39]. Formally, $tSDI$ is expressed as a ratio of the surface fire energy behavior and slope hazards against indexes of suppression opportunities, as defined in Eq. (2):

$$tSDI = \left[\frac{\sum I_{ce} + I_{slope}}{\sum(I_a + I_m + I_p + I_c)} \right] \quad (2)$$

where surface fire energy behavior (I_{ce}) is computed using FL and heat per unit area, I_{slope} denotes a factor of slope hazards, while the indexes of suppression opportunities S_{oi} are defined by accessibility (I_a), mobility (I_m), penetrability (I_p), fireline construction rate (I_c). We provide a more detailed explanation of $tSDI$ in Section S3 in the Supplementary Materials.

The metrics we use (i.e., SDI) make our approach objective. Since there is no quantitative evaluation criteria in assessing these polygons, we selected the Suppression Difficulty Index (SDI) because it is used in creating potential operation delineations (PODs) which are similar risk containment polygons. While the fire potential polygons do not explicitly provide the probability of success of containment actions, metrics such as SDI can be used to help inform and guide decision-makers who use the polygons. Users can then modify and post-process the automatically generated polygons according to operation scenarios and tactical objectives. We also highlight that SDI is only one of potential indicators. For instance, potential control location maps (which are also used to create PODs) could be another metric used for evaluation.

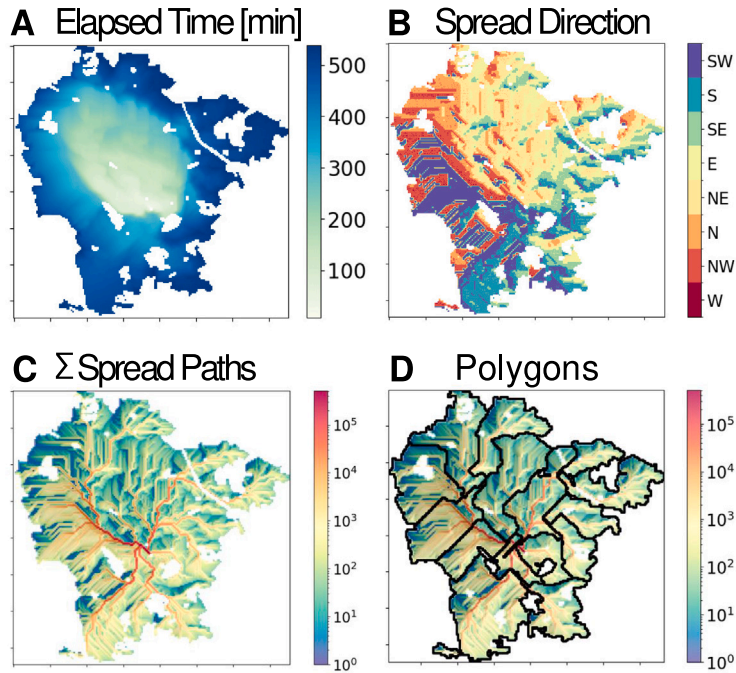


Fig. 3. Hydrology-inspired modeling of the 2024 Ciutadilla Fire. (A) Elapsed time [min]. (B) Fire spread direction. (C) Cumulative fire spread paths. (D) Fire potential polygons delineated using the Pfafstetter basin algorithm overlaid on the cumulative fire spread path raster.

4. Results

4.1. 2024 Ciutadilla fire

4.1.1. Modeling fire potential polygons

In the real fire (see Fig. 1A), the fire started to spread slowly in the agricultural fields. After a couple of hours, embers landed in forested patches and rapidly accelerated the fire's propagation to the northeast. In the Cell2Fire simulation, we apply ROS adjustment factors to reflect the fire's acceleration caused by wind conditions and embers. We adjusted the HROS and FROS by a factor of 2.8 based on in-situ measurements of wind speeds observed by fire managers. The resulting Cell2Fire simulations, depicted in Fig. 3, show the fire's spread. The simulated fire initially spread towards the north-northwest in its head direction for five hours. Subsequently, the simulated fire progressed to the northeast and ultimately jumped the highway in the last couple of hours. From the Σ fire spread paths raster (see Fig. 3C), we found major fire pathways propagating to the northwest (head direction), northeast (right flank), and several pathways to the south (back direction). Using the Σ fire spread paths raster, we delineated 15 fire potential polygons, as shown in Fig. 3D.

4.1.2. Networks of fire potential polygons for decision-making during suppression

We create a network of fire potential polygons as shown in Fig. 4A. To note, the node numbers are used for identification not enumeration, since preprocessing polygons (see Section 3.2) may eliminate and/or merge existing polygons. The ignition point is in polygon 17 and the fire propagated predominantly in the northwest direction. The thickness of the network edges is scaled by the penetration ratio. The network visualization shows several high-risk connections: the network edge in the fire's head direction (i.e., polygons 17 to 10) and in the fire's left flank (i.e., polygons 17 to 15).

Starting from polygon 17, we discover that the fastest spreading fire path is in the head direction connecting polygons 17, 10, and 1 (see Fig. 4B) due to the high wind speeds and dry surface fuels. The second fastest path started in the fire's left flank in polygons 17 to 15 (see Fig. 4C), which then spread into polygons 10 and 12. To avoid the fire from escaping beyond polygon 15, aerial retardant was dropped to slow the fire and reduce intensity.

The fire spread to the east-northeast appears less concerning. However, recall that the key objective was to prevent the fire from crossing the highway and entering the northeast (past polygons 2 and 4). Slowing the fire in advance at polygons 7 and 8 was therefore paramount to avoid this worst-case scenario. We highlight all possible edges leading to polygons 7 and 8 using dotted red lines in 4D. Tractors were used to create fire breaks by plowing the crop fields to stop the fire spread (See photo in Fig. 4D).

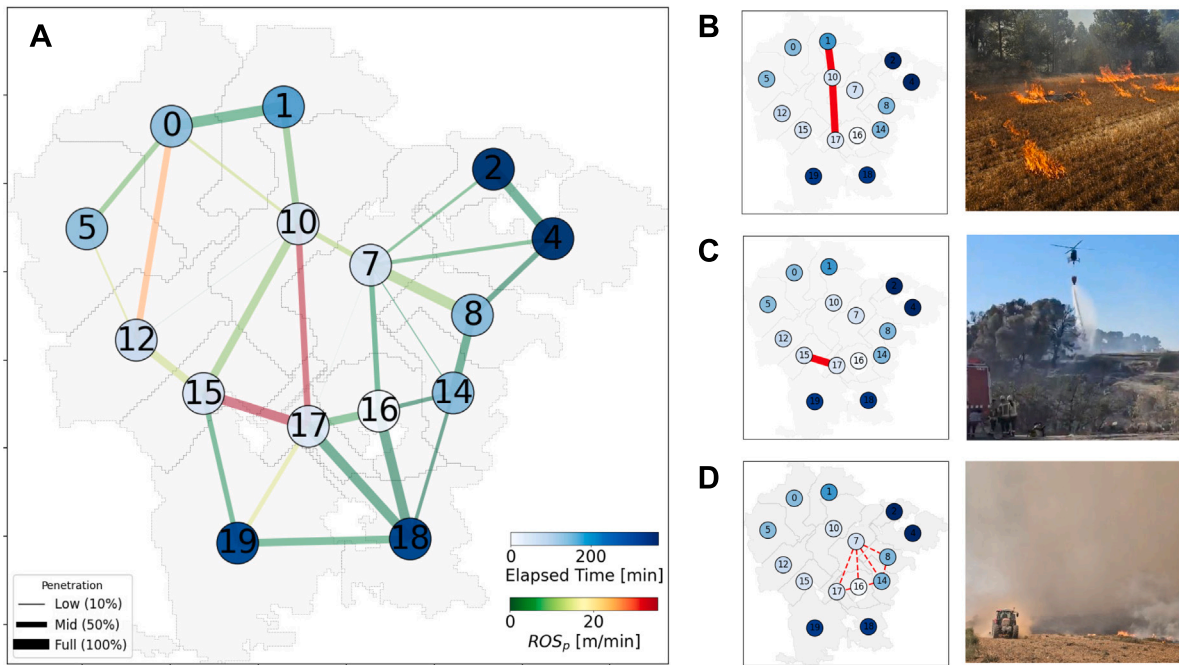


Fig. 4. Fire potential network and highlighted fire pathways. The width of the network's edges are scaled based on the penetration ratio term in Eq. (1). To note, the node numbers are used for identification not for enumeration. (A) Network visualization for fire suppression decision-making with edges weighted by ROS_p [m/min] and nodes by elapsed time [min]. (B) Fastest spreading fire path (highlighted by polygons 17, 10, 1) propelled by high winds, spotting, and fast-spreading surface fuels. (C) Fast spread westward (polygons 17 to 15) was slowed using aerial retardants to avoid opening the fire's left flank towards polygons 12 and 5. (D) Tractors created fire breaks in advance inside polygons 16 and 7 to ensure the fire would not jump the highway and spread to high-risk polygons 2 and 4. All network edges connecting to polygons 7 and 8 are shown by the dotted red lines.

4.1.3. Comparison of fire potential polygons

We compare our automatically generated fire potential polygons with the manually drawn polygons in Table 1 and display the results in Fig. 5. We generate 15 fire potential polygons with an average area of 50.75 ha and nine polygons directly overlapping the burn. In contrast, there are nine manually drawn polygons drawn with an average area of 45.15 ha and only five polygons directly overlapping the burn. In both cases, the actual burned area extends beyond the limits of the polygons due to the continuous winds pushing to the northwest. There are more polygons in the automatically generated set since we use a longer time duration for the simulation. Increasing the number of polygons may escalate the complexity of decision-making. In this case, the additional polygons in the fire's right flank (e.g., Automated polygons 2, 4, 7, 8) are helpful to anticipate potential fire behavior and realize "what-if" high-risk scenarios (e.g., Fire progresses northeast and jumps the highway).

Both sets of polygons share a low average $tSDI$ (manual: 0.154; automated: 0.186), which is expected since most fuels were surface fuels with limited terrain slope. In particular, maximum average $tSDI$ is found in the northern-most polygon (manual polygon 1 and automated polygons 0 and 1), which is more pronounced in the manually-drawn polygons (see Fig. 5B). However, at a granular level, we find high $tSDI$ in local areas, particularly near slope hazards (See Fig. S4 in Supplementary Materials). Notably, we highlight that the actual strategy was very similar to the major fire pathways in our fire potential network. First, given the high ROS_p between polygons 17 to 10 (Fig. 4B), firefighters waited for the fire to pass through polygon 10. Fire suppression was then focused on the connection between polygons 10 and 1. Second, there was a high risk of fire spread in the fire's left flank in Polygons 17 to 15 (Fig. 4C). Major aerial resources (i.e., fire retardant) were dropped to limit potential fire spread. Lastly, proactive strategies (e.g., fire breaks using tractors) were quintessential to avoid the fire from evolving into the worst-case scenario. These strategies focused on mitigating fire spread and not underestimating potential fire openings. The fire service engaged the fire's right flank later in time (at polygon–polygon connections 16 to 14; 7 to 2; and 7 to 4).

4.2. 2024 Vilanova de Meià fire: suppression tactics with prescribed burn

4.2.1. Impact of suppression interventions on modeled fire potential polygons

We simulate each scenario in Cell2Fire and compare the change in elapsed time in Fig. 6. The elapsed time from the "No Suppression" scenario (t_0) is used as the baseline to assess the impact of the different scenarios. In the "Prescribed Burn" scenario, the reduction of fuels helps slow the propagation of the fire in the polygons to the north/northeast. The fire stops at the polygon's

Table 1
Comparison of manual and automated polygons used in the Ciutadilla Fire.

Category	Manually drawn	Automated (Ours)
Number of polygons	9	15
Average area per polygon	45.15 ha	50.75 ha
Average $tSDI$ per polygon	0.154	0.186
Number of polygons over-lapping burned area	5	9

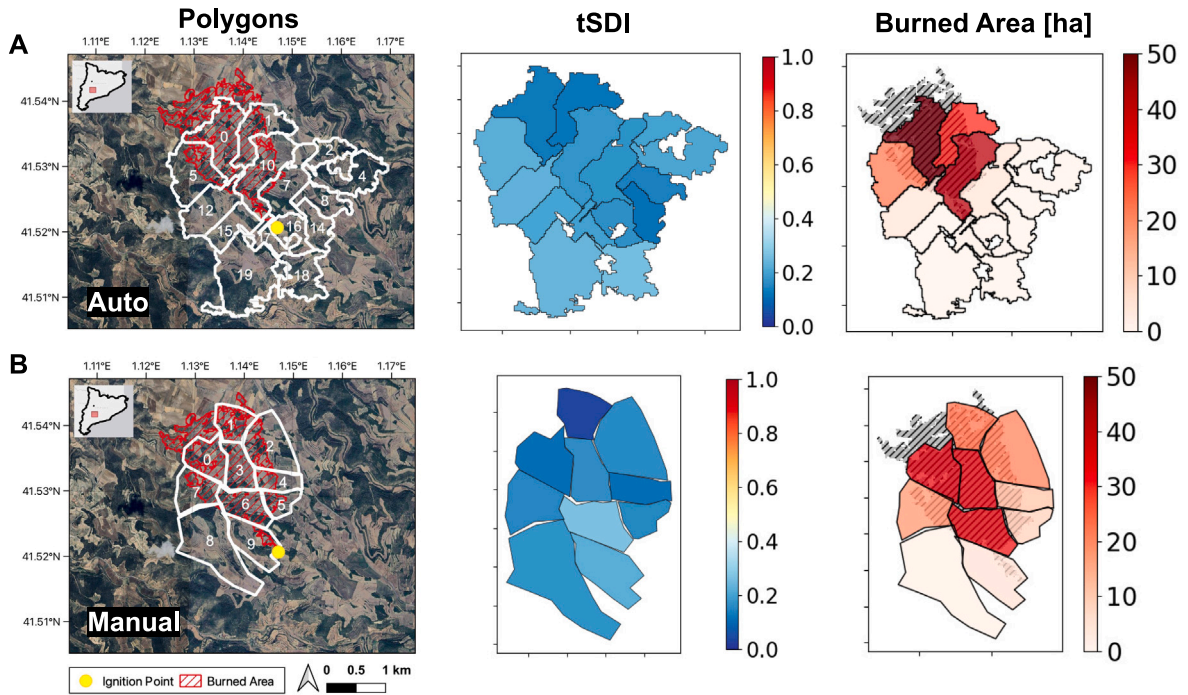


Fig. 5. Comparison of automated and manual polygons in terms of suppression difficulty and burned area for the 2024 Ciutadilla fire. (A) Map of automated polygons (white outline) shown over actual burn area (red), terrestrial suppression difficulty index ($tSDI$), and burned area per polygon. (B) Map of manual polygons drawn by fire analysts and experts (white outline) shown over actual burn area (red), $tSDI$, and burned area per polygon.

extremities in t_{rx} . In the “Reactive” scenario shown by t_r , subtle changes are observed in the polygons east and south of the fire’s right flank. Lastly, in the “Proactive” scenario shown by t_p , we see the greatest gain in elapsed time. This scenario effectively suppresses the head and left flank of the fire.

We compare the time gained from each scenario using cumulative distribution functions (CDFs) in Fig. 6B. The “Prescribed Burn” (dotted line) produces a slight rightward shift in its CDF, which reflects modest delays in fire spread. The “Reactive” scenario (blue line) shows a marginal increase in elapsed time, but minimal improvement from implementing reactive tactics. The “Proactive” scenario (red line) exhibits the greatest shift in its CDF, suggesting significant gains in elapsed time and widespread reduction in fire spread.

We display the impact of the scenarios as differences in Fig. 6C. The “Prescribed Burn” scenario ($t_{rx} - t_0$) reduces fire spread heading north/northeast. From a strategic standpoint, the prescribed burn is important to avoid the worst-case scenario (i.e., fire escaping and heading north/northeast to Montargull). However, relying on prescribed burning alone has minimal effect because the fire follows alternative pathways to the northeast polygons. The “Reactive” scenario ($t_r - t_0$) delays the fire spread to the south/southeast but with marginal impact. In contrast, the “Proactive” scenario ($t_p - t_0$) slows the fire spread considerably. The proactive tactics successfully block the fire’s progression into the northwest polygon and leverages the prescribed burn more effectively. This result is critical for decision-making during initial attack. At a glance, the fire’s right flank heading south/southeast seems urgent. However, proactive tactics are needed to avoid prolonging fire spread into an extended attack. We also examine ROS, FLI, and FL for each scenario and present probability distribution functions of the change in elapsed time in Fig. S6 of the Supplementary Materials.

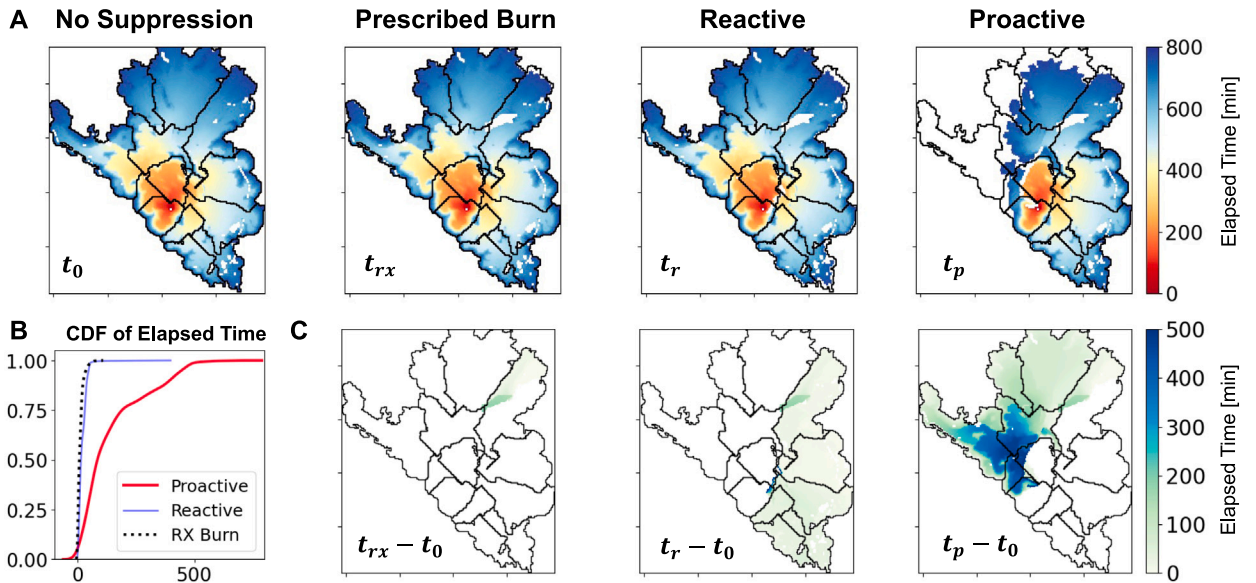


Fig. 6. Impact of suppression tactics on fire spread simulation time. (A) Comparison of elapsed time outputs without any interventions (t_0), only prescribed burn (t_{rx}), and all tactics (prescribed burn and suppression tactics S1 to S4) shown with fire potential polygons (black outline). (B) Cumulative distribution functions of the change in elapsed time for each tactic (t_{rx} and t_p) with respect to the no suppression benchmark. (C) Visualization of change in elapsed time following prescribed burn ($t_{rx}-t_0$), all reactive tactics (t_r-t_0), and all proactive tactics (t_p-t_0).

4.2.2. Impact of suppression interventions on modeled fire potential networks

We show the pre-suppression network (Fig. 7A) from the “No Suppression” scenario and post-suppression networks using the “Reactive” (Fig. 7B) and “Proactive” scenarios (Fig. 7D). Polygons can be identified by their node number. The structure of the networks changed markedly across suppression scenarios.

In the pre-suppression network, there are several network edges with high ROS_p , such as connections between polygons 9 and 4, 9 and 2, as well as 3 and 0. We find major fire pathways with high ROS_p connecting polygons 10, 9, 4; polygons 10, 6, 2, 1; and polygons 10, 6, 8. The regions of most concern are large forested areas in the north (i.e., polygons 1, 0 and 3). If the fire were to enter these polygons, suppression would become overly complex and difficult. Comparing the pre and post-suppression networks reveals a decrease in ROS_p for select connections. Considering the worst-case scenario in the northern polygons, the “Reactive” scenario helps to reduce ROS_p between Polygons 0 and 3 as well as Polygons 2 and 3. Although reactive tactics attempt to stop fire spread in the south/southeast (i.e., Polygons 8, 12, 14), the mitigation has minimal effect on ROS_p . In contrast, the “Proactive” tactics leads to a significant reduction in ROS_p for many high-risk connections. We observe reduced ROS_p in the north/northeast polygons to avoid the worst-case scenario. We also see reduced fire spread in the northwest to delay the opening of potential fire pathways.

To quantify the impact of suppression, we display the change in elapsed time across all polygons. We compute the difference between the post and pre-suppression networks in Figs. 7C and D. The “Reactive” scenario yields only a slight amount of time gained (approximately 30 min) in polygons 11, 13 and 4. In contrast, for the “Proactive” scenario, there is significant time gained after suppression. We highlight significant time gained in north-northwest polygons 4, 2, 1, 0. Polygon 4 experiences the most increase in time at 478 min, as fire barely entered the polygon. Polygons 2, 1, and 0 record the next greatest gain in time at 220, 196, and 135 min, respectively.

4.2.3. Comparison of fire potential polygons

We compare the automated fire potential polygons based on the “No Suppression” scenario with the manually drawn polygons in Table 2 and display the results in Fig. 8. We automatically generate 13 fire potential polygons with an average area of 72.55 ha and seven polygons directly overlapping the burn. In contrast, there are 12 polygons drawn manually during the real fire with an average area of 56.99 ha and eight polygons directly overlapping the burn. The average $tSDI$ is higher for the manually-drawn polygons, especially near the center where topography is highly complex (i.e., manual polygon 10 with $tSDI$ of 0.347). This polygon is in a critical area for decision-making since it is connected to multiple polygons in the north which could lead to more complex fire behavior. In the automated polygons, this region is segmented by a larger-sized polygon (i.e., automated polygon 2 with $tSDI$ of 0.257). See Fig. S7 in the Supplementary Materials for more detailed images of $tSDI$. Both sets of polygons follow the main trajectory of the fire toward the northeast. This suggests that the automated polygons could also be used to forecast the fire’s main movement.

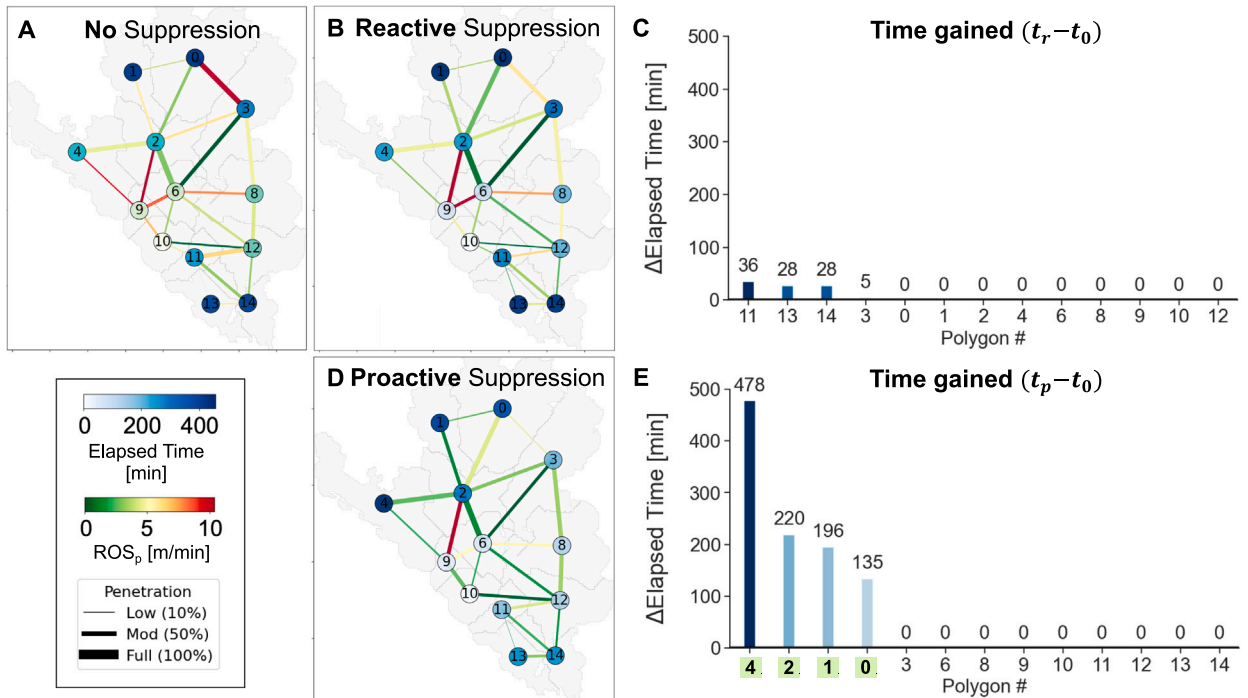


Fig. 7. Dynamic updating of networks following all tactics (i.e., prescribed burn and all four suppression tactics) with edges weighted by penetration ROS (ROS_p) [m/min] and nodes by elapsed time [min]. The width of the network’s edges are scaled based on the penetration ratio term in Eq. (1). To note, the node numbers are used for identification not for enumeration. (A) Pre-suppression network based on the “No Suppression” scenario. (B) Post-suppression network based on the “Reactive” scenario. (C) Change in elapsed time plotted in descending order of polygons with the most time gained. (D) Post-suppression network based on the “Proactive” scenario. (E) Change in elapsed time plotted in descending order of polygons with the most time gained with the top polygons highlighted in green.

Table 2
Comparison of manual and automated polygons used in the Vilanova de Meià Fire.

Category	Manually drawn	Automated (Ours)
Number of polygons	12	13
Average area per polygon	56.99 ha	72.55 ha
Average $iSDI$ per polygon	0.347	0.257
Number of polygons over-lapping burned area	8	7

5. Discussion

In this study, we develop an automatic method to generate fire potential polygons and connect them into a network to visualize risk and inform strategic decision-making. Fire potential networks help identify high-risk polygons, connections, and major fire pathways that could lead to unexpected fire openings and cascading effects. We applied our method on two wildfires during initial attack. Both fires possessed the potential of growing larger and causing devastating damage. Our results demonstrate how critical decisions had maximum impact. Mitigation and suppression tactics are implemented to dynamically update the network and visualize changes in the system. We reveal that applying proactive tactics with a prescribed burn helps to significantly reduce fire spread, earning crucial time for suppression.

5.1. Fire potential polygons for operational decision-making

Fire potential polygons provide essential risk-informed information for operational decision-making [7,15,40]. The polygons can help decision-makers understand how to manage uncertainty, identify limitations of the current fire suppression system, and raise public awareness on wildfire risks [7]. The polygons can also be used to focus on the most benefiting outcome possible at the time of suppression. In this study, we automatically generated fire potential polygons based on fire behavior. The polygons contain major fire pathways, similar to a basin containing its main tributaries. Hence, the polygons could be treated as individually or as a set of decisions. In our two case studies, we simulate for a specific set of parameters to emulate the observed fire’s conditions. However,

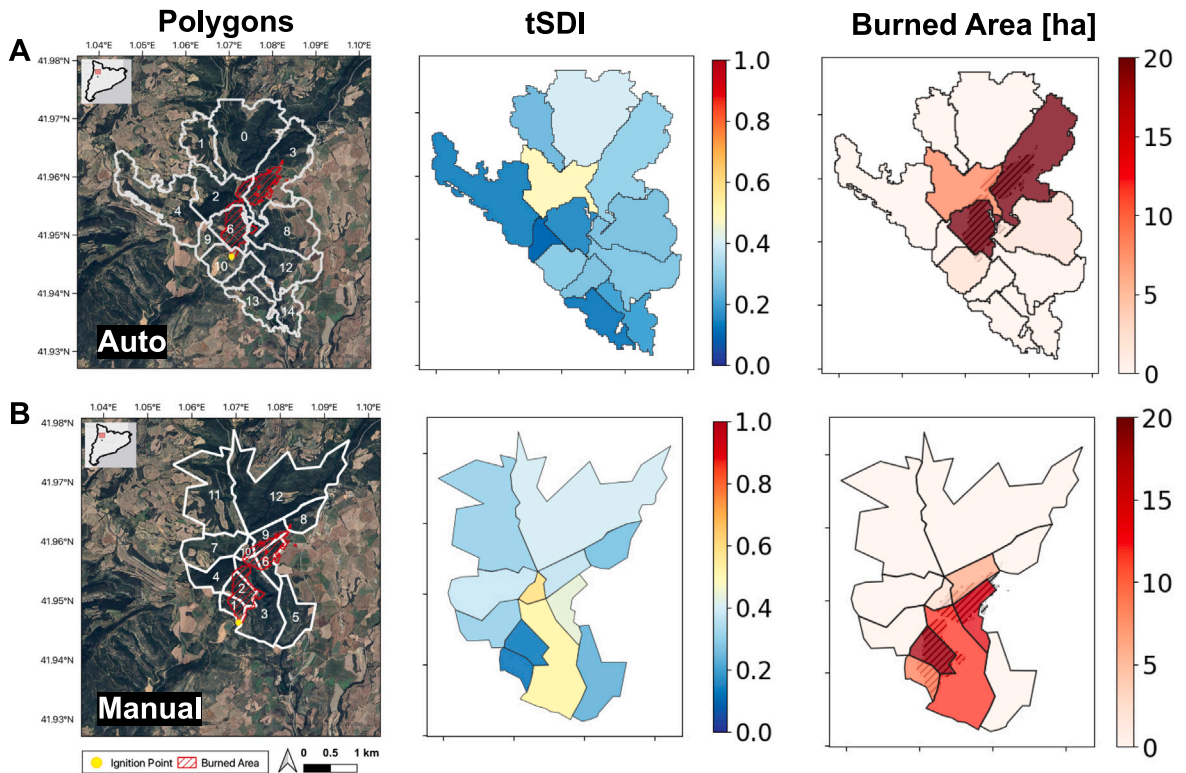


Fig. 8. Comparison of automated and manual polygons in terms of suppression difficulty and burned area for the 2024 Vilanova de Meià fire. (A) Map of automated polygons (white outline) shown over actual burn area (red), $tSDI$, and burned area per polygon. (B) Map of manual polygons drawn by fire analysts and experts (white outline) shown over actual burn area (red), $tSDI$, and burned area per polygon.

future works can apply different parameters to plan for fires under various scenarios. Scenario planning can help decision-makers anticipate different “what-if” cases. This exploration is important to help users familiarize themselves with the local landscape and potential fire behavior.

One drawback with this simulation-based approach is the reliance on existing fire spread simulators. Semi-empirical fire spread models can be limited when predicting extreme fire behavior such as spotting driven by high winds [41,42]. In this study, we apply ROS adjustment factors to compensate for this behavior in the first case study. Future fire spread models need to be updated to address this uncertainty, especially given the surge in extreme fires in recent years. Nevertheless, ROS adjustments are considered to be an effective modification for operational fire management [42–44].

Post-processing may be required to refine the polygon boundaries. Although fire spread simulations consider non-fuel areas and discontinuities, the resulting polygon boundaries may not explicitly align with specific features like roads and ridgelines. Users can manually adjust polygon boundaries to these suppression opportunities (i.e., potential control locations) according to their strategic objectives. Another consideration is integrating landscape value and high-value risk assets within polygons [18,40]. Public participation through community workshops can help to highlight key features in the landscape and prioritize polygons during operations [18]. Community engagement is crucial to build credibility and risk awareness towards more fire-adapted communities and fire-resilient landscapes [7].

This study emphasizes the need for a proactive and holistic outlook on fire suppression. However, the goal is not aggressive fire suppression and full fire exclusion from the landscape. The aim is to implement smarter, risk-informed decision-making to avoid uncontrollable fires that could lead to catastrophic damage [7,15]. Fire managers should also be wary of the consequences behind their decision-making and management of factors such as ecosystems, communities, and public health [45,46].

5.2. Fire potential polygons as networks

A key difference in our method compared to other risk-based approaches is being able to anticipate the fire’s potential movement on the landscape using fire potential networks and fire pathways. Our approach allows users to consider suppression opportunities at polygon–polygon connections as well as within polygons. In this study, we present networks weighted by different quantities of fire behavior such as ROS, FLI, and FL as well as ROS_p . Fire behavior characteristic charts [47,48] can be used to relate ROS with FLI and FL to help determine potential measures for prevention and suppression. These charts can be used with interpretations

of fire suppression measures given based on fire behavior metrics [47]. However, wildfire risk and severity can be represented by various metrics. Some metrics may be more preferred over others based on suppression priorities, tactics, and objectives. Extending from our study, users can select or customize networks according to their needs. In addition, future works can leverage network topology to build metrics that may provide richer information regarding the fire's behavior. For example, network-based metrics like betweenness centrality have frequently been used to model important fire pathways [49,50]. Downstream protection value is another metric that measures importance by integrating ecosystem values with fire behavior from Cell2Fire simulations [51,52].

In the case studies, our method identifies key major fire pathways that led to important decisions during fire suppression. Many of these key pathways aligned with the real fire's propagation. Fire pathways can also be extracted using different criteria, and have also been produced using methods like graph theory [50,53] and electric circuit theory [54–56].

The networks in this study can be extended into existing risk-based modeling approaches as well. For instance, PODs have been used to plan for wildfire risk mitigation and management but do not consider the fire's potential movement between the delineated regions. Besides, PODs were mainly developed for planning and management strategies rather than real-time suppression and operations [13]. Response PODs were developed to integrate fire spread outputs from MTT simulations. However, the resulting POD polygons are macro-polygons [57] and may be too large to effectively track fire spread [16,27]. One consideration is adding connectivity to PODs, which could help users better understand the potential spread of fire within and between PODs. Connected PODs could then be used to inform decisions on resource allocation, strategy deployment, and vulnerability analysis. Future works could explore the integration of the network building approach in this study with PODs or other existing spatial units of fire management. Integrating fire pathways with risk-informed frameworks like PODs have also been suggested in other studies [27,56].

6. Conclusion

Wildfires are complex and dynamic phenomena that pose significant challenges to fire management and suppression. In this study, we present an automatic method to generate fire potential polygons and networks to support fire suppression strategies. Our method adapts basin delineation to fire spread simulations and automatically generates fire potential polygons. These polygons are connected and modeled as networks weighted by fire behavior. Through the network, users can identify critical fire pathways, anticipate potential fire behavior, and evaluate the impact of suppression tactics. In the Ciutadilla fire, we demonstrate this modeling process and provide critical insights on potential high-risk fire pathways. In the Vilanova de Meià fire, we implement a previous prescribed burn and actual suppression tactics via Cell2Fire to analyze the impact of reactive and proactive strategies. Socio-political pressure pushed for reactive strategies to stop immediate risks at the time. Fire managers designed proactive strategies from a more holistic view (aided by our fire potential polygons and network) to avoid losing control of the fire. Our simulation results conclude that the tactics used in the proactive strategy yield substantially more time and effectively reduce fire spread. Stemming from this study, future works should focus on advancing the proposed approach by applying the method in other wildfires, regions, and scenarios. We also encourage refining polygon boundaries, experimenting with various fire behavior attributes to characterize the connected networks, and integrating landscape asset values through community workshops and expert knowledge.

CRedit authorship contribution statement

Minho Kim: Writing – review & editing, Writing – original draft, Visualization, Software, Methodology, Investigation, Formal analysis, Data curation, Conceptualization. **Marc Castellnou:** Writing – review & editing, Supervision, Methodology, Formal analysis, Conceptualization. **Marta C. González:** Writing – review & editing, Supervision, Project administration, Methodology, Funding acquisition, Formal analysis, Conceptualization.

Funding

The authors acknowledge the support of C3.ai through the grant Multiscale analysis for Improved Risk Assessment of Wildfires facilitated by Data and Computation.

Declaration of competing interest

The authors declare that they have no known competing financial interests or personal relationships that could have appeared to influence the work reported in this paper.

Acknowledgments

The authors acknowledge the support of the Catalan Fire Service for accommodation and access to the wildfires during suppression operations. Thank you to the firefighters, managers, and practitioners who provided valuable feedback and insight. The authors acknowledge the support of C3.ai through the grant Multiscale Analysis for Improved Risk Assessment of Wildfires Facilitated by Data and Computation. The authors also acknowledge the support of the Pau Costa Foundation. This study was made possible with gift funding received by the University of California, Berkeley Institute of Urban & Regional Development (IURD) in the College of Environmental Design from The Lau Fund for Just Climate Futures. The authors would like to thank the Lau family for its support of university-based research, and for the funding received for this project.

Appendix A. Supplementary data

Supplementary material related to this article can be found online at <https://doi.org/10.1016/j.ijdrr.2025.105853>.

Data availability

The Landscape data used for fire spread simulations was acquired from PREVINCAT (<https://previncat.ctfc.cat/>). Weather data was downloaded from Meteorological Service of Catalonia (<https://www.meteo.cat/observacions/xema/dades>). For fire spread simulations, Cell2Fire can be accessed from (<https://github.com/fire2a/C2F-W>). Python libraries used for the basin delineation were adopted from pysheds (<https://github.com/mbartos/pysheds>) as well as PyFlwDir (<https://github.com/Deltares/pyflwdir>). Case study data and codes are available at <https://github.com/humnetlab/firepolygons>.

References

- [1] J. Radke, Modeling fire in the wildland–urban interface: Directions for planning, in: *Living on the Edge*, vol. 6, Emerald Group Publishing Limited, 2007, pp. 183–210.
- [2] D.M. Bowman, C.A. Kolden, J.T. Abatzoglou, F.H. Johnston, G.R. van der Werf, M. Flannigan, Vegetation fires in the Anthropocene, *Nat. Rev. Earth Environ.* 1 (10) (2020) 500–515.
- [3] R.D. Collins, R. de Neufville, J. Claro, T. Oliveira, A.P. Pacheco, Forest fire management to avoid unintended consequences: A case study of Portugal using system dynamics, *J. Environ. Manag.* 130 (2013) 1–9.
- [4] J. San-Miguel-Ayanz, J.M. Moreno, A. Camia, Analysis of large fires in European Mediterranean landscapes: Lessons learned and perspectives, *Forest Ecol. Manag.* 294 (2013) 11–22.
- [5] S. Modugno, H. Balzter, B. Cole, P. Borrelli, Mapping regional patterns of large forest fires in Wildland–Urban Interface areas in Europe, *J. Environ. Manag.* 172 (2016) 112–126.
- [6] F. Schug, A. Bar-Massada, A.R. Carlson, H. Cox, T.J. Hawbaker, D. Helmers, P. Hostert, D. Kaim, N.K. Kasraee, S. Martinuzzi, et al., The global wildland–urban interface, *Nature* 621 (7977) (2023) 94–99.
- [7] M. Castellnou, N. Prat-Guitart, E. Arilla, A. Larrañaga, E. Nebot, X. Castellarnau, J. Vendrell, J. Pallàs, J. Herrera, M. Monturiol, et al., Empowering strategic decision-making for wildfire management: avoiding the fear trap and creating a resilient landscape, *Fire Ecol.* 15 (2019) 1–17.
- [8] M.R. Kreider, P.E. Higuera, S.A. Parks, W.L. Rice, N. White, A.J. Larson, Fire suppression makes wildfires more severe and accentuates impacts of climate change and fuel accumulation, *Nat. Commun.* 15 (1) (2024) 2412.
- [9] D.M. Molina-Terrén, G. Xanthopoulos, M. Diakakis, L. Ribeiro, D. Caballero, G.M. Delogu, D.X. Viegas, C.A. Silva, A. Cardil, Analysis of forest fire fatalities in southern Europe: Spain, Portugal, Greece and Sardinia (Italy), *Int. J. Wildland Fire* 28 (2) (2019) 85–98.
- [10] M. Castellnou, J. Pagés, A. Larrañaga, M. Piqué, Mapa de risc D'incendi tipus de catalunya (Map of Wildfires in Catalonia Using Fire Types Concept), 2010.
- [11] M. Desmond, Making firefighters deployable, *Qual. Sociol.* 34 (2011) 59–77.
- [12] C.J. Dunn, D.E. Calkin, M.P. Thompson, Towards enhanced risk management: planning, decision making and monitoring of US wildfire response, *Int. J. Wildland Fire* 26 (7) (2017) 551–556.
- [13] M.P. Thompson, C.D. O'Connor, B.M. Gannon, M.D. Caggiano, C.J. Dunn, C.A. Schultz, D.E. Calkin, B. Pietruszka, S.M. Greiner, R. Stratton, et al., Potential operational delineations: new horizons for proactive, risk-informed strategic land and fire management, *Fire Ecol.* 18 (1) (2022) 17.
- [14] E. Arango, P. Jiménez, M. Nogal, H.S. Sousa, M.G. Stewart, J.C. Matos, Enhancing infrastructure resilience in wildfire management to face extreme events: Insights from the Iberian Peninsula, *Clim. Risk Manag.* 44 (2024) 100595.
- [15] E. Arilla, M. Bachfischer, X. Castellarnau, J. Cespedes, M. Castellnou, J. Castellví, E. Dalmau, L. Estivill, A. Ferragut, A. Larrañaga, M. Miralles, E. Nebot, J. Pagés, P. Pallàs, M. Rosell, B. Ruiz, Piloting the adaptation of methodology of forest fire potential polygons, 2023, p. 20, <http://dx.doi.org/10.5281/zenodo.7991283>, Deliverable D1.3. FIRE-RES project.
- [16] B. Granda, J. León, B. Vitoriano, J. Hearne, Decision support models and methodologies for fire suppression, *Fire* 6 (2) (2023) 37.
- [17] F.R. y Silva, C.D. O'Connor, M.P. Thompson, J.R.M. Martínez, D.E. Calkin, Corrigendum to: Modelling suppression difficulty: current and future applications, *Int. J. Wildland Fire* 29 (8) (2020) 752–752.
- [18] G. Gamboa, I. Otero, C. Bueno, H. Ballart, L. Camprubí, G. Canaleta, G. Tolosa, M. Castellnou, et al., Participatory multi-criteria evaluation of landscape values to inform wildfire management, *J. Environ. Manag.* 327 (2023) 116762.
- [19] M. Rodrigues, M. Zúñiga Antón, F. Alcasena, P. Gelabert, C. Vega-García, Integrating geospatial wildfire models to delineate landscape management zones and inform decision-making in Mediterranean areas, *Saf. Sci.* 147 (2022) 105616.
- [20] M.A. Finney, Fire growth using minimum travel time methods, *Can. J. Forest Res.* 32 (8) (2002) 1420–1424.
- [21] J.L. Conner, D.A. Falk, S.R. Yool, R.R. Parmenter, Modeling fire pathways in montane grassland-forest ecotones, *Fire Ecol.* 14 (2018) 17–32.
- [22] C. Pais, J. Carrasco, D.L. Martell, A. Weintraub, D.L. Woodruff, Cell2Fire: A cell-based forest fire growth model to support strategic landscape management planning, *Front. For. Glob. Chang.* 4 (2021) 692706.
- [23] R.E. Keane, S.A. Drury, E.C. Karau, P.F. Hessburg, K.M. Reynolds, A method for mapping fire hazard and risk across multiple scales and its application in fire management, *Ecol. Model.* 221 (1) (2010) 2–18.
- [24] B.M. Gannon, Y. Wei, M.P. Thompson, Mitigating source water risks with improved wildfire containment, *Fire* 3 (3) (2020) 45.
- [25] T. Blaschke, Object based image analysis for remote sensing, *ISPRS J. Photogramm. Remote Sens.* 65 (1) (2010) 2–16.
- [26] S. Lang, S. Kienberger, D. Tiede, M. Hagenlocher, L. Pernkopf, Geons-domain-specific regionalization of space, *Cartogr. Geogr. Inf. Sci.* 41 (3) (2014) 214–226.
- [27] Y. Wei, M.P. Thompson, E. Belval, B. Gannon, D.E. Calkin, C.D. O'Connor, Comparing contingency fire containment strategies using simulated random scenarios, *Nat. Resour. Model.* 34 (1) (2021) e12295.
- [28] J. Nowosad, T.F. Stepinski, Extended SLIC superpixels algorithm for applications to non-imagery geospatial rasters, *Int. J. Appl. Earth Obs. Geoinf.* 112 (2022) 102935.
- [29] J.H. Scott, R.E. Burgan, Standard Fire Behavior Fuel Models: a Comprehensive Set for Use with Rothermel's Surface Fire Spread Model, US Department of Agriculture, Forest Service, Rocky Mountain Research Station, 2005.
- [30] J.R. Gonzalez-Olabarria, J. Carrasco, C. Pais, J. Garcia-Gonzalo, D. Palacios-Meneses, R. Mahaluf-Recasens, O. Porkhum, A. Weintraub, A fire spread simulator to support tactical management decisions for mediterranean landscapes, *Front. For. Glob. Chang.* 6 (2023) 1071484.
- [31] M. Kim, C. Pais, M.C. Gonzalez, Fire spread simulations using Cell2Fire on synthetic and real landscapes, *Sci. Rep.* 15 (1) (2025) 25173.

- [32] J. Carrasco, C. Pais, F. Soto, D. Palacios, R. Mahaluf, F.d.l. Barra, H. Gilabert, G. Alfaro, A. Miranda, M. Castillo, et al., C2F k: An open-source wildfire simulator based on Cell2Fire and the Chilean KITRAL system, 2023, Available At SSRN 4384499.
- [33] A. Duane, M. Pique, M. Castellnou, L. Brotons, Predictive modelling of fire occurrences from different fire spread patterns in Mediterranean landscapes, *Int. J. Wildland Fire* 24 (3) (2015) 407–418.
- [34] M. Bartos, *Pysheds: Simple and fast watershed delineation in python*, 2020, URL <https://Github.Com/Mdbartos/Pysheds>.
- [35] M. Huang, S. Jin, A methodology for simple 2-D inundation analysis in urban area using SWMM and GIS, *Nat. Hazards* 97 (1) (2019) 15–43.
- [36] K.L. Verdin, J.P. Verdin, A topological system for delineation and codification of the Earth's river basins, *J. Hydrol.* 218 (1–2) (1999) 1–12.
- [37] S. Linke, B. Lehner, C. Ouellet Dallaire, J. Ariwi, G. Grill, M. Anand, P. Beames, V. Burchard-Levine, S. Maxwell, H. Moidu, et al., Global hydro-environmental sub-basin and river reach characteristics at high spatial resolution, *Sci. Data* 6 (1) (2019) 283.
- [38] C.D. O'Connor, M.P. Thompson, F. Rodríguez y Silva, Getting ahead of the wildfire problem: Quantifying and mapping management challenges and opportunities, *Geosciences* 6 (3) (2016) 35.
- [39] F.R. y Silva, J.R.M. Martínez, A. González-Cabán, A methodology for determining operational priorities for prevention and suppression of wildland fires, *Int. J. Wildland Fire* 23 (4) (2014) 544–554.
- [40] I. Otero, M. Castellnou, I. González, E. Arilla, L. Castell, J. Castellví, F. Sánchez, J.Ø. Nielsen, Democratizing wildfire strategies. Do you realize what it means? insights from a participatory process in the Montseny region (Catalonia, Spain), *PLoS One* 13 (10) (2018) e0204806.
- [41] P.L. Andrews, Current status and future needs of the BehavePlus fire modeling system, *Int. J. Wildland Fire* 23 (1) (2013) 21–33.
- [42] A. Cardil, S. Monedero, P. SeLegue, M.Á. Navarrete, S. de Miguel, S. Purdy, G. Marshall, T. Chavez, K. Allison, R. Quilez, et al., Performance of operational fire spread models in California, *Int. J. Wildland Fire* 32 (11) (2023) 1492–1502.
- [43] A. Cardil, S. Monedero, C.A. Silva, J. Ramirez, Adjusting the rate of spread of fire simulations in real-time, *Ecol. Model.* 395 (2019) 39–44.
- [44] S. Yoo, W.H. Kang, J. Song, Wildfire spread prediction using geostationary satellite observation data and directional ROS adjustment factor, *J. Environ. Manag.* 372 (2024) 123358.
- [45] C.A. Schultz, M.P. Thompson, S.M. McCaffrey, Forest service fire management and the elusiveness of change, *Fire Ecol.* 15 (2019) 1–15.
- [46] M. Essen, S. McCaffrey, J. Abrams, T. Paveglio, Improving wildfire management outcomes: shifting the paradigm of wildfire from simple to complex risk, *J. Environ. Plan. Manag.* 66 (5) (2023) 909–927.
- [47] P.L. Andrews, R.C. Rothermel, *Charts for Interpreting Wildland Fire Behavior Characteristics*, vol. 131, US Department of Agriculture, Forest Service, Intermountain Forest and Range ..., 1982.
- [48] P.L. Andrews, *How to Generate and Interpret Fire Characteristics Charts for Surface and Crown Fire Behavior*, (253) US Department of Agriculture, Forest Service, Rocky Mountain Research Station, 2011.
- [49] B.A. Aparício, J.M. Pereira, F.C. Santos, C. Bruni, A.C. Sá, Combining wildfire behaviour simulations and network analysis to support wildfire management: A mediterranean landscape case study, *Ecol. Indic.* 137 (2022) 108726.
- [50] A.C. Sá, B. Aparício, A. Benali, C. Bruni, M. Salis, F. Silva, M. Marta-Almeida, S. Pereira, A. Rocha, J. Pereira, Coupling wildfire spread simulations and connectivity analysis for hazard assessment: a case study in Serra da Cabreira, Portugal, *Nat. Hazards Earth Syst. Sci.* 22 (12) (2022) 3917–3938.
- [51] C. Pais, J. Carrasco, P.E. Moudio, Z.J.M. Shen, Downstream protection value: Detecting critical zones for effective fuel-treatment under wildfire risk, *Comput. Oper. Res.* 131 (2021) 105252.
- [52] P. Elimbi Moudio, C. Pais, Z.J.M. Shen, Quantifying the impact of ecosystem services for landscape management under wildfire hazard, *Nat. Hazards* 106 (2021) 531–560.
- [53] H. Mahmoud, A. Chulahwat, Unraveling the complexity of wildland urban interface fires, *Sci. Rep.* 8 (1) (2018) 9315.
- [54] M.E. Gray, B.G. Dickson, A new model of landscape-scale fire connectivity applied to resource and fire management in the Sonoran Desert, USA, *Ecol. Appl.* 25 (4) (2015) 1099–1113.
- [55] M.E. Gray, B.G. Dickson, Applying fire connectivity and centrality measures to mitigate the cheatgrass-fire cycle in the arid west, USA, *Landsc. Ecol.* 31 (2016) 1681–1696.
- [56] E.K. Buchholtz, J. Kreitler, D.J. Shinneman, M. Crist, J. Heinrichs, Assessing large landscape patterns of potential fire connectivity using circuit methods, *Landsc. Ecol.* 38 (7) (2023) 1663–1676.
- [57] Y. Wei, M.P. Thompson, J.R. Haas, G.K. Dillon, C.D. O'Connor, Spatial optimization of operationally relevant large fire confine and point protection strategies: Model development and test cases, *Can. J. Forest Res.* 48 (5) (2018) 480–493.